

Article

The Synthesis and Morphology of a Perfluoroalkyl Oligosiloxane@SiO₂ Resin and Its Performance in Anti-Fingerprint Coating

Qiufeng An *, Zhujun Lyu, Wenchao Shangguan, Bianli Qiao and Pengwei Qin

Key Laboratory of Auxiliary Chemistry & Technology for Chemical Industry, Shaanxi University of Science and Technology, Xi'an 710021, China; lyuzhujun@163.com (Z.L.); shangguan_wenchao@163.com (W.S.); qbl420@126.com (B.Q.); qpw1005204720@163.com (P.Q.)

* Correspondence: anqf@sust.edu.cn; Tel.: +86-29-86573337

Received: 27 December 2017; Accepted: 8 March 2018; Published: 9 March 2018

Abstract: In order to improve the hydro- and oleo-phobic properties of anti-fingerprint coating, novel oligosiloxane intermediate bearing perfluorodecyl/octyl and triethoxy silylethylene groups were synthesized; then, a series of nano-hybrid perfluoroalkyl oligosiloxane resins (FSi@SiO₂) were synthesized using the hydrolysis and condensation of FVPS with tetraethylorthosilicate. The chemical structure, morphology, and performance of FSi@SiO₂ were investigated. The results indicate that the FSi@SiO₂ is a nano hybrid fluorinated polysiloxane resin with mean particle sizes of 200–400 nm. And under nanoparticles and perfluoroalkyl groups bonded in the resin, FSi@SiO₂ not only showed a micro rough morphology in atomic force microscopy observation but also could provide the treated substrates with excellent hydro- and oleo-phobicity. As a result, the water and oil contact angles reached 120.3° and 87.5° on the treated glass, respectively; meanwhile, fingerprints were easily cleaned without any stains.

Keywords: morphology; nano-hybrid; perfluoroalkyl oligosiloxane; hydrophobic; oleophobic; transparent; touchscreen

1. Introduction

As we all know, when a finger touches a glass surface, a fingerprint contamination layer remains. This undesired residue is predominantly water but also contains skin oils, sweat, and cosmetics, resulting in an oily liquid [1]. Once deposited on a transparent surface, such as the touchscreen of a mobile phone, iPad, or pocket computer, it decreases optical transmittance and hinders visibility [2,3]. Therefore, a study on how to keep touchscreens free of fingerprints and make them easier to clean should probably focus on developing transparent hydrophobic and oleophobic coatings; this has become an urgent and primary problem that needs to be solved [4], especially as electronic devices and wearable electronics have developed rapidly. Thus, the demand for anti-fingerprint materials is expected to increase greatly in the next few years [5].

Super-hydrophobic phenomena in nature have provided human beings with effective and feasible models (such as lotus leaves and water striders) for the creation of anti-fingerprint coatings. The lotus leaf's self-cleaning effect is due to the unique geometrical structure and hydrophobic waxy materials of the surface, which offer promising applications in hydro- and oleo-phobicity, self-cleaning, and anti-fouling [6]. Thus, combining nano-particles with low-surface-energy materials such as fluorinated or organosilicon compounds via physical blending or chemical bonding could mimic the lotus leaf structure in hydro- and oleo-phobic coating fabrication [7]. A number of reports have been developed on the preparation of nanoparticles with SiO₂ [8–10]. However, among the low-surface-energy materials, only perfluoroalkyl compounds and polymers are ideal

candidates for improving both dirt resistance and hydrophobic and oleophobic (i.e., amphiphobic) properties, due to their characteristic low surface tension, low wettability, and low adhesiveness of stains to the coating [11–14]. Zhang et al. [15] successfully formed superhydrophobic coatings by introducing fluorinated alkyl silane functionalized silica nanoparticles into polydimethylsiloxane resin. Ling et al. [16] used amino-silane-treated glass as the substrate and perfluoro-decyltrichloro-silane for a subsequent vacuum evaporation process, and transparent superhydrophobicity was achieved. Wang et al. [17] published a study describing the production of durable superhydrophobic coated surfaces based on tridecafluoro-octyl-triethoxy-silane and a modification of SiO₂ nanoparticles with polydimethylsiloxane.

Using nanoparticles plus low-surface-energy materials via blending could rapidly create a superhydrophobic coating with a water contact angle >150° and a sliding angle <10° [18–20]. However, the nanoparticles contained in the system easily fall off the coating surface. Besides, cracking, less transmittance, and poor durability to rubbing are still challenges that are related to the practical use of such fabricated coatings. Chemically bonding or robustly combining nanoparticles with perfluoropolymer or perfluorosilsesquioxane may solve the problem and provide better performance (such as rigidity and transparency) for the fabricated coating.

Since the anti-fingerprint coating must have the characteristics of smoothness, rigidity, transparency, and thinness (usually 2–3 μm) in industry applications, and in order to obtain the expected amphiphobic properties in coating fabrication, a novel intermediate perfluoro-1H,1H,2H,2H-decyl/octyl and trimethoxysilylethylene cyclotetrasiloxane (FVPS) and nano SiO₂ bonded with perfluorodecyl/octyl oligosiloxane (FSi@SiO₂) resin was designed and synthesized. On the basis of this, a strong hydrophobic and oleophobic coating with easy-to-clean properties was built.

2. Experiment

2.1. Materials and Reagents

1H,1H,2H-perfluoro-1-decene (PFDE) and 1H,1H,2H-perfluoro-1-octene (PFOE) were purchased from Fuxin Hengtong Chemical Co., Fuxin, China. Vinyl triethoxysilane (VTES) was supplied by Qufu Chenguang Chemical Co., Qufu, China. 1,3,5,7-tetramethylcyclotetrasiloxane (D₄^H) and methyl-silicone (MQ) resin were provided by China National Bluestar (Group) Co., Beijing, China. Platinum complex catalyst (KP22) and trifluoroethanol (TFE) were obtained from Shanghai Zhongzixing Chemical Co. (Shanghai, China) and Shanghai Haiqu Chemical Co. (Shanghai, China), respectively. Dibutyl tin diacetate was supplied by Hangzhou Guibao Chemical Co., Hangzhou, China. Tetraethylorthosilicate (TEOS), petroleum ether, acetone, and hydrochloric acid were purchased from Xi'an Chemical and Reagent Co., Xi'an, China. All reagents were used as received.

2.2. Synthesis of Hydro- and Oleo-Phobic Intermediate

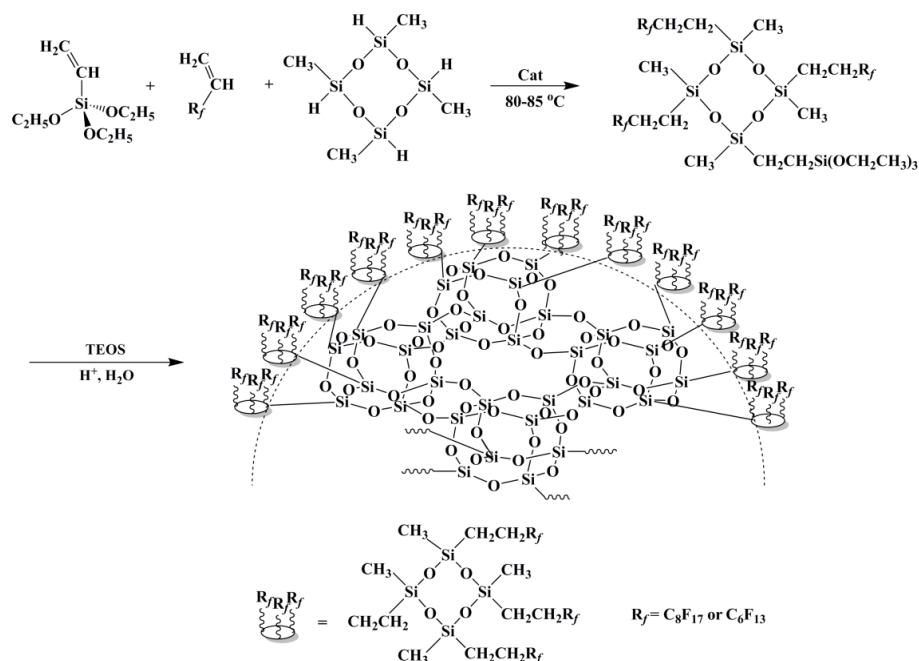
In a three-neck flask equipped with a thermometer, a mechanical stirrer, and a reflux condenser, PFDE or PFOE, VTES, and D₄^H were added in a mole ratio of PFDE/PFOE:VTES:D₄^H of about 3:1:1. After being stirred for 10 min, the mixture was heated to 80 °C under nitrogen protection, and then a catalytic amount of platinum complex catalyst KP22 was added. The mixture was maintained at 80 °C for 10 h, and the low-boiling-point substances were removed at reduced pressure. Finally, a transparent to slightly brown fluid, the intermediate, 1,3,5,7-tetramethyl-3,5,7-tri(perfluorodecyl/octyl)-1-triethoxysilylethylene cyclotetrasiloxane, was obtained and noted as FVPS.

2.3. Synthesis of Nano SiO₂ Hybrid Fluorinated Alkyl Oligosiloxane Resin

In another three-neck flask equipped with a thermometer, a mechanical stirrer, and a reflux condenser, FVPS and TEOS were added in turn and mixed in a mole ratio of FVPS:TEOS of 1:3, then the solvent TFE was added in a mass ratio of TFE to (FVPS + TEOS) of about 10:1. The mixture was stirred and heated to 40 °C, then hydrochloric acid and deionized water were added in dropwise

fashion. After the reaction was carried out for 10 h, the solvent and low-boiling-point substances were removed via reduced pressure distillation at 85–90 °C and 260 mm Hg until the resin mass concentration reached 60%–70%. Finally, a clear solution containing nano SiO₂ hybrid fluorinated alkyl oligosiloxane (FSi@SiO₂) resin was obtained (illustrated as Scheme 1).

In addition, the SiO₂ sol prepared from TEOS, following the same route as above, was used as a reference.



Scheme 1. Schematic illustration of synthetic procedure of FSi@SiO₂ resin.

2.4. Preparation of the FSi@SiO₂ Anti-Fingerprint Coating

Pretreatment of the glass or mobile touchscreen: Prior to the coating treatment, pieces of glass or mobile touchscreen were washed with detergent solution and deionized water, then ultrasonically in acetone for 30 min to remove oil residue and dirt. After being dried at 100–105 °C for 20 min, the cleaned glass or touchscreen was etched by plasma in air atmosphere for 20–30 s, while the gas flow rate was controlled at about $1.69 \times 10^{-1} \text{ Pa}\cdot\text{m}^3/\text{s}$.

Coating preparation: A flow chart of the preparation of anti-fingerprint coating is displayed in Scheme 2. First, the 60%–70% FSi@SiO₂ resin was dissolved and diluted with acetone to form a mass concentration of 0.8% treating solution, then the 30% methyl-MQ silicon resin solution, which was dissolved by petroleum ether (17 wt % in treating solution), and a catalytic quantity of dibutyl tin diacetate (about 2–4 drops in 100 mL solution) were added and fully stirred. Then, the etched glass was fixed on an experimental platform and sprayed with the above treating solution to form a coating. After being kept at room atmosphere for 2–3 min, the coated glass was placed in an oven and cured at 130 °C for 25–30 min. Finally, the FSi@SiO₂ coating anchored on the glass substrate was obtained and kept in a desiccator until it was used.



Scheme 2. Flow chart of preparation of anti-fingerprint coating.

2.5. Characterization

Fourier-transform infrared spectroscopy (FT-IR) of the intermediate FVPS and the target FSi@SiO₂ was recorded on a Bruker VECTOR-22 spectrometer (Bruker, Ettlingen, Baden-Württemberg, Germany), KBr liquid film method. The nanoparticle sizes in the FSi@SiO₂ solution were measured by Malvern Nano-ZS particle sizer (Malvern Instruments Co., Malvern, Worcestershire, UK). Transmission electron microscopy (TEM, Hitachi, Tokyo, Japan) of the FSi@SiO₂ resin was performed on an H-600 transmission electronic microscope with an acceleration voltage of 200 kV. The samples were stained with 2% phosphotungstic acid solution. SEM measurement was carried out on a TM-1000 scanning electron microscope (Hitachi, Tokyo, Japan), and morphologic photographs were taken at a magnification of 1000×. Atomic force microscopy (AFM) images were obtained with a Nanoscope IIIA AFM (Agilent Technologies, Palo Alto, CA, USA) in tapping mode. All scanning was performed at 22 °C in air with relative humidity of 48%. The chemical structure of the FSi@SiO₂ film on the treated glass was investigated by an Axis Ultra X-ray photoelectron spectrum (XPS) made in Kratos, Manchester, UK. Static water contact angles (WCAs) on the glass treated with FSi@SiO₂ were determined via the sessile drop method on a JC2000A contact angle goniometer (Shanghai Zhong Chen Digital Co., Shanghai, China) at 20 °C. The liquid volume was 5 μL, and the average of 5 readings from different regions of the same sample was used as the final contact angle of each sample. Spectral transmittances between 300 and 800 nm wavelength were measured using a Cary 5000 ultraviolet-visible spectrophotometer (Agilent Co., Palo Alto, CA, USA), with blank glass as a control. Abrasion resistance analysis was done using LKY-II wet abrasion scrub tester (Hongwei Co., Dongguan, Guangdong, China) with 500 gram weight; cotton cloth was used as abrasion material.

3. Results and Discussion

3.1. About Design and Synthesis of FSi@SiO₂

In synthesizing the intermediate and target products, bonding perfluoroalkyl and trialkoxyl silyl groups into the oligosiloxane structure could impart the intermediate with excellent amphiphobicity and reactivity similar to perfluoroalkyl trialkoxysilane. Introducing the rigid Q (quaternary siloxane) segments or nano-rough structures into the fluorinated polysilsesquioxane/polysiloxane could make the resin generate an inorganic-organic hybrid and improve the rigidity and transmittance of the FSi@SiO₂. Meanwhile, the more fluorinated groups introduced in the oligosiloxane, the stronger the hydro- and oleo-phobic properties of the intermediate and target FSi@SiO₂. In view of this, the mole ratio of PFDE/PFOE:VTES:D₄^H was designed to be 3:1:1 in reaction. To ensure that the Si-H residue from D₄^H was completely consumed in the synthesis of FVPS, slightly excessive PFDE/PFOE and VTES were replenished before the end of hydrosilylation.

An effective method of producing nano-hybrid is to hydrolyze perfluoroalkyl silane with 4 to 6 functional silanes, the nano source material in acidic, or alkali conditions. Therefore, in this experiment, the intermediate FVPS was hydrolyzed with TEOS in a mole ratio of 1:3 (FVPS:TEOS) at a pH of about 4–5. However, to avoid the cyclotetrasiloxane oligomer opening the ring in hydrolysis, the reaction temperature was maintained at around 40 °C, which may be suitable for the alkoxy silyl to convert into Si-OHs and condense into the target FSi@SiO₂ resin.

3.2. Characterization of FVPS and FSi@SiO₂

In the following procedures, FVPS prepared from PFDE and FSi@SiO₂ prepared from FVPS:TEOS in a mole ratio of 1:3 were used as samples to investigate the structure, morphology, and performance of the intermediate and target resins.

Figures 1 and 2 show the FT-IR and proton nuclear magnetic resonance (¹H-NMR) spectra of the intermediate FVPS and target FSi@SiO₂ resins. As is obvious in Figure 1, the stretching and distortion vibration peaks due to Si-O and C-F bonding, resulting from the skeleton and side groups of FVPS, respectively, occurred at 1099 (ν_{Si-O}), 1212 (ν_{C-F}), and 780 (ν_{C-F}) cm⁻¹. Adsorption at 3400 cm⁻¹ that

belonged to Si–OH groups appeared in a weak peak in FSi@SiO₂ spectrum (Figure 1b), indicating that a large number of Si–OH groups originate from the hydrolysis of FVPS and TEOS reacted with each other and condensed in the target product. In addition, FVPS exhibited characteristic stretching peaks at 2991 and 2878 cm⁻¹, belonging to the C–H groups.

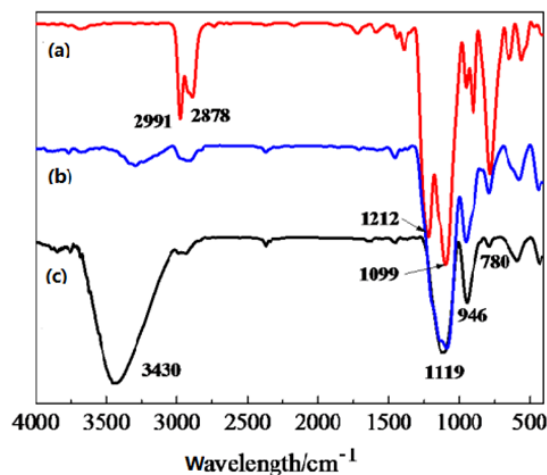


Figure 1. FT-IR spectra of (a) FVPS; (b) FSi@SiO₂; and (c) SiO₂ sol.

Figure 2 shows the ¹H-NMR spectra of FSi@SiO₂ and its intermediate FVPS. The chemical shift signal due to Si–CH₃ (aH) appeared at δ_H 0.15, and bH and b'H belonging to Si–CH₂ occurred at δ_H about 0.74. The peak signal at δ_H 2.05 should be derived from the CH of the methylene bonded with perfluorodecyl/octyl (–CH₂R_f, R_f = C₈F₁₇ or C₆F₁₃). Meanwhile, the strong signals at δ_H 1.22 and 3.83 in FVPS that belonged to SiOCH₂CH₃ clearly vanished from the spectrum of FSi@SiO₂ after the hydrolysis.

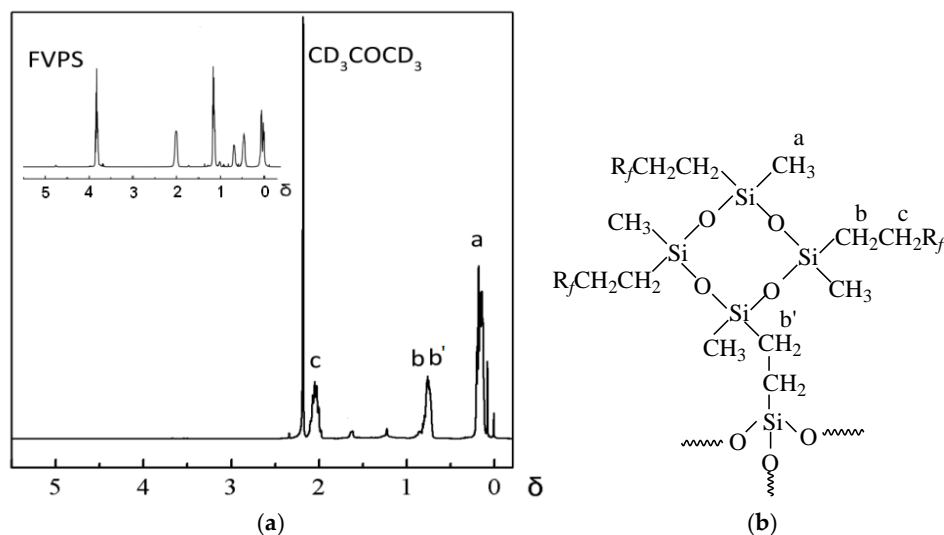


Figure 2. ¹H-NMR spectra of FSi@SiO₂ (a) and intermediate FVPS (b).

3.3. State and Particle Size Distribution of the FSi@SiO₂ Resin Solution

In synthesizing FSi@SiO₂, the bigger the nanoparticles combined in the resin, the rougher of the coating fabricated from the FSi@SiO₂ [21]. However, the big nano particles have an unfavorable impact on the transmittance and smoothness of the coating, especially as the big particles load on

the perfluoro oligosiloxane coating surface. Thus, the nano particle size distribution of the FSi@SiO₂ solution was investigated.

Figure 3 shows the TEM photograph, state, and particle size distribution (PSD) of the FSi@SiO₂ resin solution. Figure 3a shows the TEM of FVPS resin. Compared with the FVPS and FSi@SiO₂, obviously, FSi@SiO₂ was a nano-hybrid resin (Figure 3b), although it was clear in appearance (Figure 3c). The nanoparticles in the FSi@SiO₂ solution were about 200–400 nm (Figure 3c) and seemed to have a quasi-spherical core-shell structure. In addition, the average particle was about 321.3 nm in diameter, which accorded well with the TEM result.

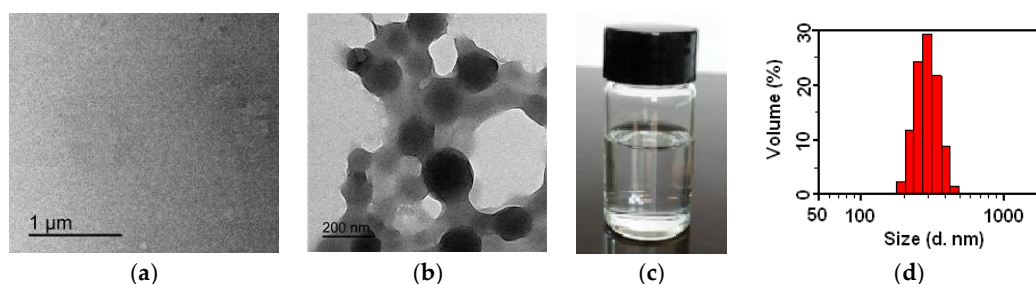


Figure 3. FVPS and FSi@SiO₂ resin: (a) TEM photograph, FVPS; (b) TEM photograph, FSi@SiO₂; (c) resin state, FSi@SiO₂; and (d) particle size distribution, FSi@SiO₂.

The XRD spectra are illustrated in Figure 4. The spectra of SiO₂ sol and FSi@SiO₂ did not show the characteristic crystal peak of SiO₂; instead, they all displayed significant dispersive peaks. Thus, SiO₂ sol and FSi@SiO₂ all have an amorphous structure. In Figure 4b,c, evidently, at $2\theta = 24.6^\circ$, the dispersive peaks signals were stronger than those of the FVPS. It is easy to see that a large number of amorphous nanoparticles were formed in the SiO₂ hybrid perfluoro oligosiloxane resin.

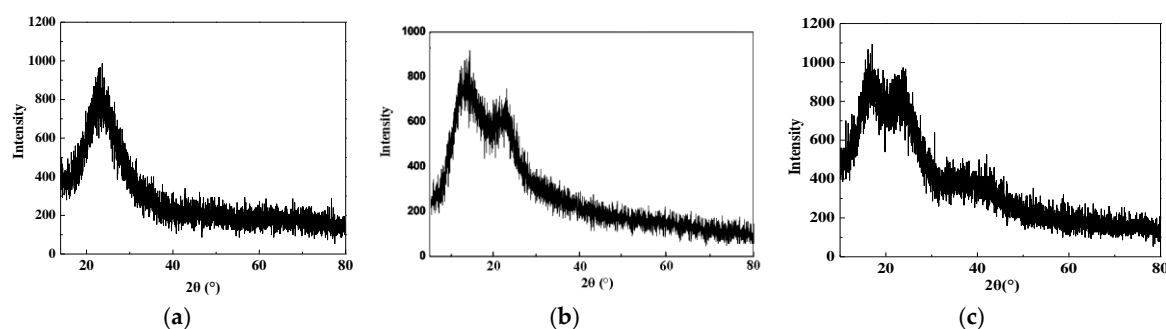


Figure 4. XRD spectra: (a) SiO₂ sol; (b) FVPS; and (c) FSi@SiO₂.

3.4. Morphology and Hydrophobic Properties of the FSi@SiO₂ Anti-Fingerprint Coating on Substrates

Hydrophobicity, oleophobicity, and other performance properties of a solid surface are determined by chemical composition and morphology of the solid surface [22–24]. Moreover, micro-/nano-rough structure is an essential and primary factor in preparation of super-hydrophobic surfaces [25]. Therefore, exploring the macro- and micro-morphology of the FSi@SiO₂ resin [26] will help us to better understand why the coating exhibits strong hydro- and oleo-phobicity and reveals the anti-fingerprint mechanism of FSi@SiO₂.

SEM and AFM provide two effective methods for observing the morphology of a coating on the μm -to-nanometer scale [27]. As shown as in Figures 5b and 6c,d, the FSi@SiO₂ formed a rugged and uneven coating on a toughened glass and silicon wafer substrate. As the data scale was 81.69 nm and the scanning field was $4 \times 4 \mu\text{m}^2$, a lot of nanoparticles emerged in the FSi@SiO₂ coating. Additionally, under the influence of these particles, the root mean square roughness of the FSi@SiO₂ reached about

1.190 nm, which should have a positive contribution to the amphiphobicity of the fabricated coating. However, as shown in the SEM and AFM images of the FVPS (Figures 5a and 6a,b), a relatively smooth coating was formed on the wafer.

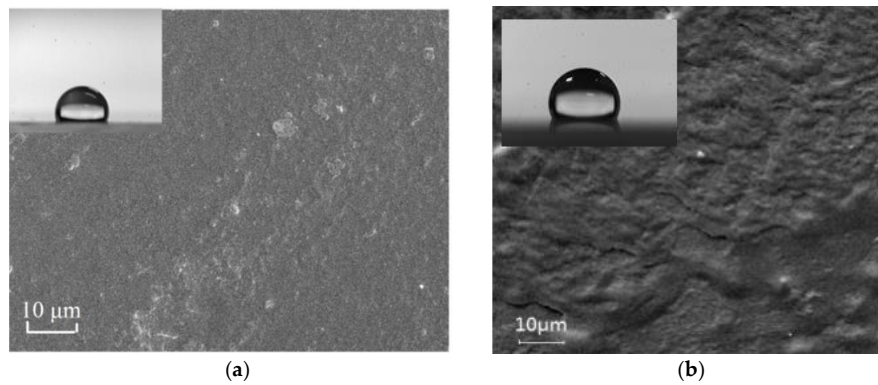


Figure 5. SEM photographs of FVPS and FSi@SiO₂ coating on toughened glass: (a) FVPS, WCA = 110.2°; (b) FSi@SiO₂, WCA = 120.3°.

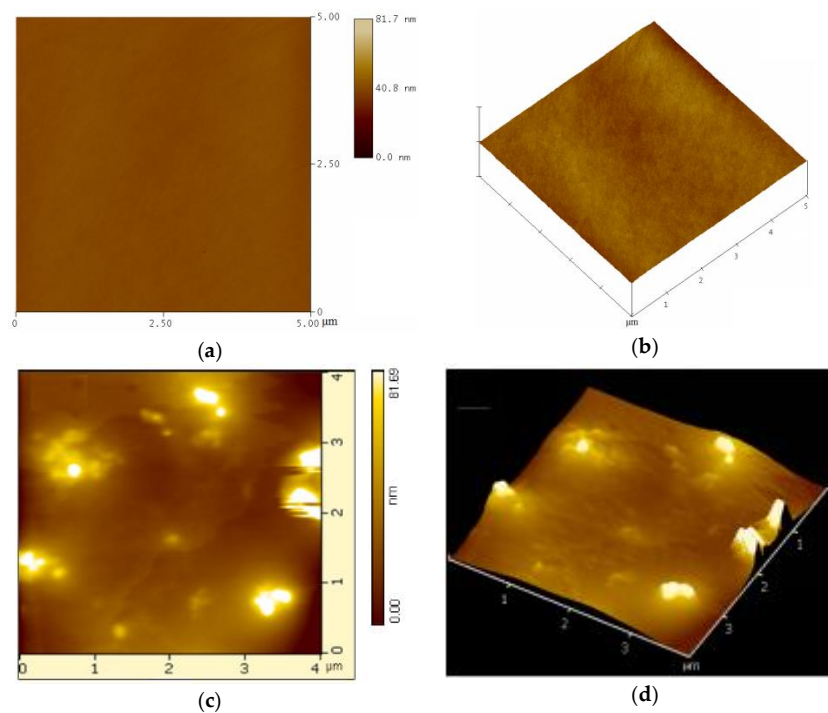


Figure 6. AFM images of FVPS and FSi@SiO₂ coating on a silicon wafer: (a) flattened, FVPS; (b) 3D, FVPS; (c) flattened, FSi@SiO₂; and (d) 3D, FSi@SiO₂.

Figure 7a–d exhibits the wide-scanning XPS and high-resolution F1s, C1s, Si2p spectra of FSi@SiO₂.

Apparently, four strong characteristic peaks, belonging to fluorine, oxygen, carbon, and silicon, occurred at binding energies of about 687.00 (F1s), 530.00 (O1s), 283.00 (C1s), and 100.00 (Si2p) eV, respectively. It is clear that the C1s spectra could be curve-fitted into four peak components at binding energies of about 287.10, 285.80, 289.03, and 292.80 eV, respectively, which were attributable to the C–C/C–H, C–Si, C–F(CF₂), and C–F(CF₃) and consistent with those reported in [28]. The Si2p spectra in Figure 7c illustrated the peaks at 99.80 eV for Si and 103.32 eV for organo/inorgano Si–O bonds. Also, the strong feature signals duo to F1s split into two peaks at 688.00 and 687.43 eV (shown in Figure 7d), indicating a large amount of organo C–F bondage in the FSi@SiO₂ coating.

Figure 8a–d exhibits the wide-scanning XPS and high-resolution F1s, C1s, Si2p spectra of FVPS. Compared with the FSi@SiO₂, spectra are not very different.

The presence of a large amount of C–Fs cooperating with nanoparticles, as well as their aggregates, provides the FSi@SiO₂ with a good opportunity not only to have a transparent appearance (Figure 9) but also to possess strong hydrophobicity in coating fabrication, though the thickness of the FSi@SiO₂ coating was 3 μm. As a result, a strong hydro- and oleo-phobic coating prepared from the FSi@SiO₂ resin was obtained in our experiment. As shown in Figure 9, the water droplets not only could stand on the treated touchscreen but could also easily slide from the treated surface.

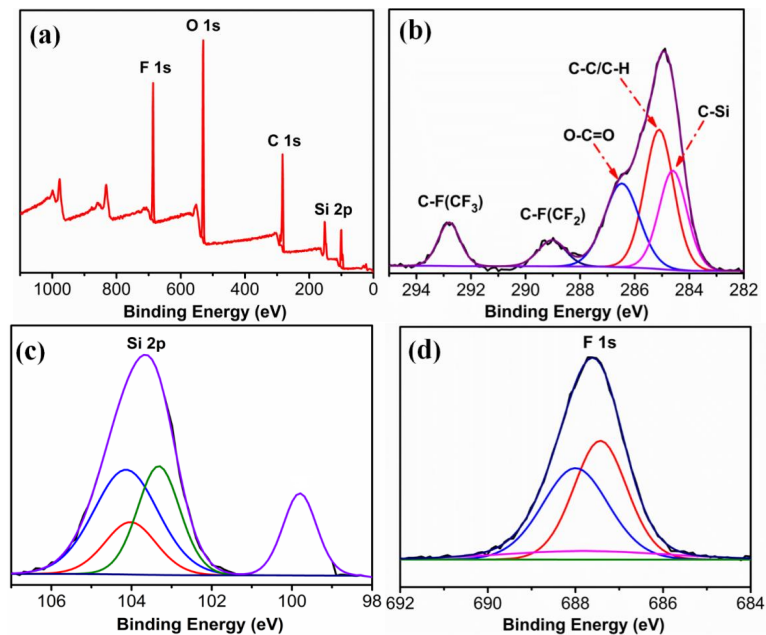


Figure 7. XPS and high-resolution spectra of FSi@SiO₂ on the silicon wafer: (a) wide scanning; (b) C1s; (c) Si2p; and (d) F1s.

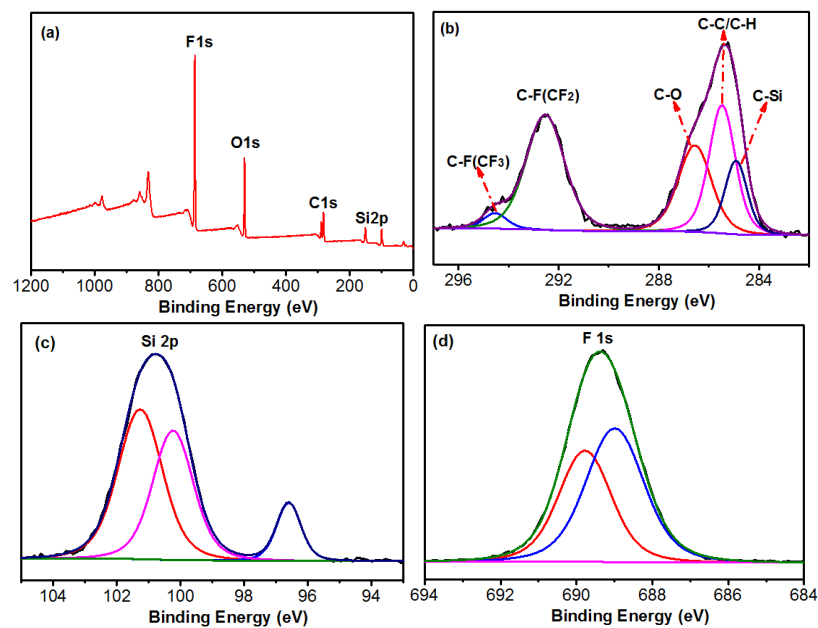


Figure 8. XPS and high-resolution spectra of FVPS on the silicon wafer: (a) wide scanning; (b) C1s; (c) Si2p; and (d) F1s.



Figure 9. Hydrophobicity of FSi@SiO₂ coating on mobile phone screen.

3.5. Performance of the FVPS and FSi@SiO₂

The FSi@SiO₂ treating solution was prepared from FVPS bearing C₈F₁₇ groups and TEOS in a mole ratio of 1:3. The mass concentration of treating solutions was 0.8 wt %. The temperature and curing time of the coating was 130 °C × 25 min, and the coating method was spraying. The result is shown in Table 1.

Table 1. Performance of the FSi@SiO₂ coating.

Treating Solutions	wt %	WCA (°)	OCA (°)	T %	Appearance	Abrasion Resistant/Cycles	AF property
FSi@SiO ₂	0.8	120.3	87.5	95	transparent	5000	☉
FVPS	0.8	110.2	65.8	92	transparent	5000	–

Notes: The mass of FSi@SiO₂ resin and FVPS resin per 100 g acetone solvent; OCA: oil contact angle (sunflower oil); T: transmittance; AF: anti-fingerprint; ☉: easily cleaned. WCA and OCA of the coating prepared from TEOS and FVPS bearing C₆F₁₃ were 120.1° and 84.9°, respectively.

Table 1 indicates that the WCA and OCA of the FSi@SiO₂ coating became bigger than the control, the untreated glass. In addition, the WCA and OCA of the FSi@SiO₂ coating (thickness of about 3 μm) reached 120.3° and 87.5°, respectively, which were significantly lower than the water contact angle of the same resin coated on the etched wafer by the dipping method (WCA = 150.3°; Figure 10). Obviously, the layer thickness has some passive effect on the hydrophobicity. Moreover, the abrasion resistance is determined by evaluating the change in a static WCA. The glass treated with FVPS without TEOS hydrolysis also showed durable hydro- and oleo-phobicity with slightly lower WCA and OCA compared with that treated with FSi@SiO₂. These control tests indicate that the high superhydrophobicity is a result of the silica nanoscale roughness imparted by the silica nanoparticles, rather than just the perfluoroalkyl (FVPS) alone. As can be seen from Figure 11, after the 5000 abrasion cycles resistance test, the WCA of FVPS and FSi@SiO₂ coating changed slightly, and the WCA decreased 2.9° and 0.8°, respectively. The abrasion resistance simulates actual damage. Although the WCA reduced with a further increase of the abrasion cycles, the treated glasses withstood at least 5000 cycles of abrasion damage without losing their hydrophobicity. Compared with the Dow Corning® (Midland, MI, USA) 2604 Coating, via the same test method, the Dow Corning new anti-fingerprint coating after 5000 abrasion cycles, the WCA decreased 1°, but the FSi@SiO₂ coating only decreased 0.8° [29], which manifests the FSi@SiO₂ coating durability meet the basic practical applications. Apparently, chemically bonding nanoparticles with perfluorosilsesquioxane can endow glasses with highly durable coating. Furthermore, from Figure 12, it can be seen that the FSi@SiO₂ and FVPS resin coatings both have good transmittance (>90% as compared with the control—the blank touchscreen glass). In addition, for the fingerprint test, Figure 13 clearly shows that the fingerprint on blank glass is much more conspicuous than on the FSi@SiO₂ coating. Also, the fingerprints on blank glass were difficult to clean, but the fingerprints on FSi@SiO₂ coating were easily wiped off. Therefore, FSi@SiO₂ treating solution has good anti-fingerprint properties.

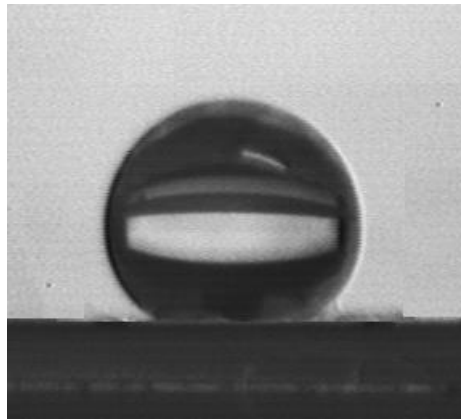


Figure 10. Silicon wafer treated with FSi@SiO₂ in dipping method, WCA = 150.3°.

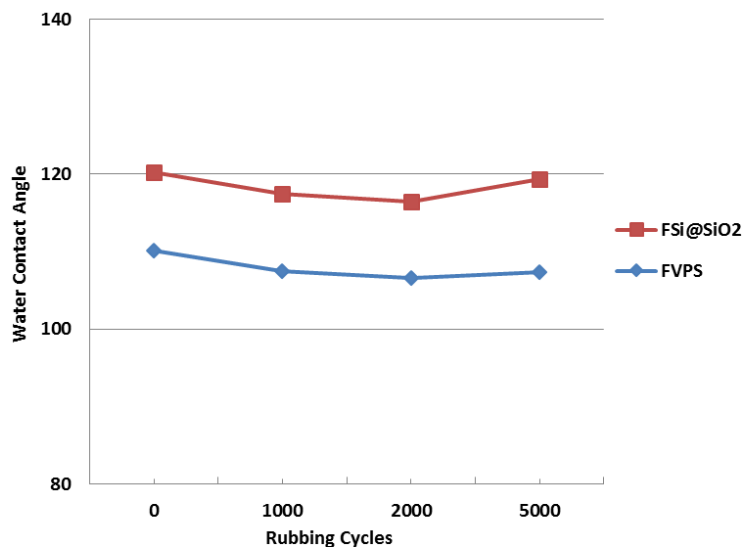


Figure 11. Impact of Rubbing Durability on Water Contact Angles.

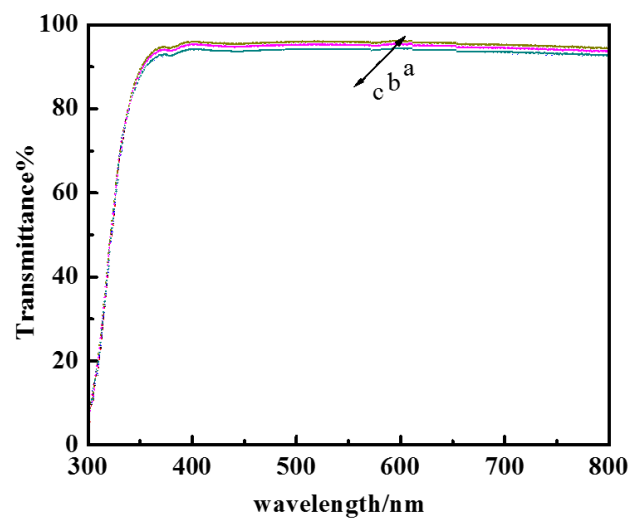


Figure 12. Transmittance of the coatings: (a) blank; (b) FSi@SiO₂; (c) FVPS.

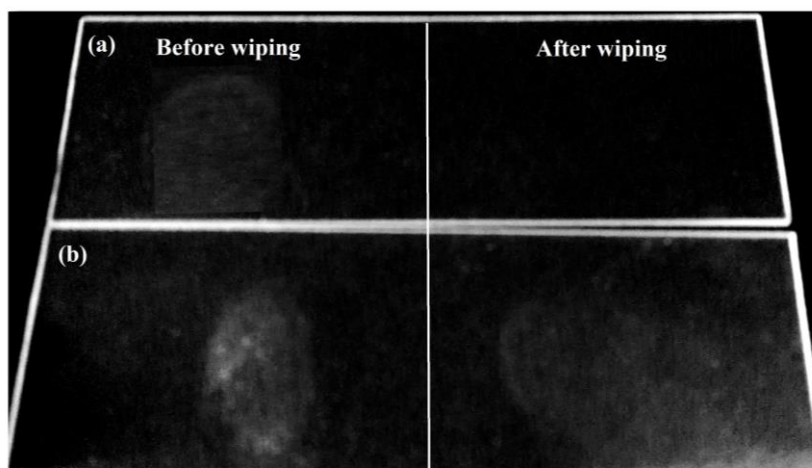


Figure 13. Fingerprint test: (a) coating with FSi@SiO₂ treating solution; (b) blank.

4. Conclusions

By hydrosilylation of D₄^H with PFDE/PFOE and VTES, an intermediate cyclotetrasiloxane oligomer bearing perfluoroalkyl and trimethoxy silylethylene groups was synthesized. Based on FVPS, a series of perfluoro nano-SiO₂ hybrid polysiloxane oligomer resins were synthesized by the hydrolysis and condensation of FVPS with TEOS. An investigation of TEM and AFM indicated that nanoparticles were combined in the FSi@SiO₂ resin. Under the influence of nano particles and their aggregates, as well as the perfluorodecyl/octyl, FSi@SiO₂ not only showed relatively rough morphology but also good hydro- and oleo-phobic properties on the treated substrate. As a result, the WCA on the FSi@SiO₂ coating reached 120.3°, and the OCA reached 87.5°, since the low-surface-energy perfluorodecyl/octyl groups aggregated on the coating surface. Contact angle and visual analysis of artificial fingerprints, both before and after wiping, most readily demonstrated that the FSi@SiO₂ treating solution had good hydrophobicity and oleophobicity, and fingerprints were easily cleaned without any stains. A fingerprint mainly contains water and oils; therefore, the transparent FSi@SiO₂ coating showed good anti-fingerprint properties, and such good durability may be useful for various functional applications.

Acknowledgments: This work was supported by a major project of the Ministry of Science and Technology of China [2017YFB0307700], a major project of scientific and technological coordination from Shaanxi Province [2015KTCL01-14], and an industrialization cultivation project of Shaanxi Provincial Education Department [16JF004].

Author Contributions: Qiufeng An, Zhujun Lyu, Wenchao Shangguan, and Bianli Qiao conceived and designed the experiments; Zhujun Lyu, Wenchao Shangguan, and Bianli Qiao performed the experiments; Zhujun Lyu and Wenchao Shangguan analyzed the data; Zhujun Lyu and Pengwei Qin contributed reagents/materials/analysis tools (Origin 8.0, Nanoscope analysis, XPS peak 4.1, MestReNova, JC2000A contact angle goniometer and Excel); and Qiufeng An and Zhujun Lyu wrote the paper.

Conflicts of Interest: The authors declare no conflict of interest.

References

1. Thomas, G.L.; Reynoldson, T.E. Some observation on fingerprint deposits. *J. Phys D Appl. Phys.* **1975**, *8*, 724–729. [[CrossRef](#)]
2. Uhlmann, P.; Frenzel, R.; Voit, B.; Mock, U.; Szyszka, B.; Schmidt, B.; Ondratschek, D.; Gochermann, J.; Roths, K. Research agenda surface technology: Future demands for research in the field of coatings materials. *Process Org. Coat.* **2007**, *58*, 122–126. [[CrossRef](#)]
3. Colaiacovo, F.; Tortora, S.; Totoreto, L.; Mauro, S.; Salamone, G. Method for Restoring or Executing an Anti Fingerprint Coating onto Sheets of Stainless Steel. U.S. Patent No. 20,090,087,649, 2 April 2009.
4. Siriviryanun, A.; Imae, T. Anti-fingerprint properties of non-fluorinated organosiloxane self-assembled monolayer-coated glass surfaces. *Chem. Eng. J.* **2014**, *246*, 254–259. [[CrossRef](#)]

5. Scruton, B.; Robins, B.W.; Blott, B.H. The deposition of fingerprint films. *Appl. Phys.* **1975**, *8*, 714–723. [[CrossRef](#)]
6. Choi, H.; Park, K.C.; Lee, H.; Crouzier, T.; Rubner, M.F.; Cohen, R.E.; Barbastathis, G.; McKinley, G.H. Superoleophilic titania nanoparticle coatings with fast fingerprint decomposition and high transparency. *ACS Appl. Mater. Interfaces* **2017**, *9*, 8354–8360. [[CrossRef](#)] [[PubMed](#)]
7. Parale, V.G.; Mahadik, D.B.; Mahadik, S.A. OTES modified transparent dip coated silica coatings. *Ceram. Int.* **2013**, *39*, 835–840. [[CrossRef](#)]
8. Xu, Q.; Wang, J.; Sanderson, S. Superhydrophobic and transparent coatings based on removable polymeric spheres. *J. Mater. Chem.* **2009**, *19*, 655–660. [[CrossRef](#)]
9. Bae, G.Y.; Min, B.G.; Jeong, Y.G.; Lee, S.C.; Jang, J.H.; Koo, G.H. Superhydrophobicity of cotton fabrics treated with silica nanoparticles and water-repellent agent. *J. Colloid Interface Sci.* **2009**, *337*, 170–175. [[CrossRef](#)] [[PubMed](#)]
10. Aslanidou, D.; Karapanagiotis, I.; Panayiotou, C. Tuning the wetting properties of siloxane-nanoparticle coatings to induce superhydrophobicity and superoleophobicity for stone protection. *Mater. Des.* **2016**, *108*, 736–744. [[CrossRef](#)]
11. Li, J.; Weng, R.; Di, X.; Yao, Z. Gradient and weather resistant hybrid super-hydrophobic coating based on fluorinated epoxy resin. *Appl. Polym. Sci.* **2014**, *10*, 40955. [[CrossRef](#)]
12. Basu, B.J.; Dinesh, V.K.; Anandan, C. Surface studies on superhydrophobic and oleophobic polydimethylsiloxane–silica nanocomposite coating system. *Appl. Surf. Sci.* **2012**, *261*, 807–814. [[CrossRef](#)]
13. Navarrini, W.; Tortelli, V.; Colaianna, P.; Abusleme, J.A. Perfluorodioxoles, the Preparation Process Thereof, and Homopolymers and Copolymers Therefrom. U.S. Patent No. 5,646,223, 8 July 1997.
14. Yang, H.; Cheng, Y.; Xiao, F. Thermal stable superhydrophobic polyphenylsilsesquioxane/nanosilica composite coatings. *Appl. Surf. Sci.* **2011**, *258*, 1572–1580. [[CrossRef](#)]
15. Zhang, Z.; Ge, B.; Men, X.; Li, Y. Mechanically durable, superhydrophobic coatings prepared by dual-layer method for anti-corrosion and self-cleaning. *Colloids Surf. A Physicochem. Eng. Asp.* **2016**, *490*, 182–188. [[CrossRef](#)]
16. Wang, Y.; Shi, Y.; Pan, L.; Yang, M.; Peng, L.; Zong, S.; Yu, G. Multifunctional superhydrophobic surfaces templated from innately microstructured hydrogel matrix. *Nano Lett.* **2014**, *14*, 4803–4809. [[CrossRef](#)] [[PubMed](#)]
17. Teisala, H.; Tuominen, M.; Kuusipalo, J. Superhydrophobic coatings on cellulose-based materials: Fabrication, properties, and applications. *Adv. Mater. Interfaces* **2013**, *1*, 1300026. [[CrossRef](#)]
18. Vecellio, M. Opportunities and developments in fluoropolymeric coatings. *Prog. Org. Coat.* **2000**, *40*, 225–242. [[CrossRef](#)]
19. Wang, H.; Fang, J.; Cheng, T.; Ding, J.; Qu, L.; Dai, L.; Wang, X.; Lin, T. One-step coating of fluoro-containing silica nanoparticles for universal generation of surface superhydrophobicity. *Chem. Commun.* **2008**, *7*, 877–879. [[CrossRef](#)] [[PubMed](#)]
20. Song, X.; Zhai, J.; Wang, Y.; Jiang, L. Fabrication of superhydrophobic surfaces by self-assembly and their water-adhesion properties. *Phys. Chem.* **2005**, *109*, 4048–4052. [[CrossRef](#)] [[PubMed](#)]
21. Karunakaran, R.G.; Lu, C.; Zhang, Z.; Yang, S. Highly transparent superhydrophobic surfaces from the coassembly of nanoparticles (≤ 100 nm). *Langmuir* **2011**, *27*, 4594–4602. [[CrossRef](#)] [[PubMed](#)]
22. Bravo, J.; Zhai, L.; Wu, Z.; Cohen, R.E.; Rubner, M.F. Transparent superhydrophobic films based on silica nanoparticles. *Langmuir* **2007**, *23*, 7293–7298. [[CrossRef](#)] [[PubMed](#)]
23. Zhu, X.; Zhang, Z.; Xu, X. Facile fabrication of a superamphiphobic surface on the copper substrate. *J. Colloid Interface Sci.* **2012**, *367*, 443–449. [[CrossRef](#)] [[PubMed](#)]
24. Ha, J.W.; Park, I.J.; Lee, S.B. Hydrophobicity and sliding behavior of liquid droplets on the fluorinated latex films. *Macromolecules* **2005**, *38*, 736–744. [[CrossRef](#)]
25. Xiong, S.; Guo, X.; Li, L.; Wu, S.; Chu, P.; Xu, Z. Preparation and characterization of fluorinated acrylate copolymer latexes by miniemulsion polymerization under microwave irradiation. *J. Fluor. Chem.* **2010**, *131*, 417–425. [[CrossRef](#)]
26. Yang, T.; Yao, L.; Peng, H.; Cheng, S.; Park, I. Characterization of a low-wettable surface based on perfluoroalkyl acrylate copolymers. *J. Fluor. Chem.* **2006**, *127*, 1105–1110. [[CrossRef](#)]

27. Cui, X.; Zhong, S.; Yan, J.; Wang, C.; Zhang, H.; Wang, H. Synthesis and characterization of core-shell SiO₂-fluorinated polyacrylate nanocomposite latex particles containing fluorine in the shell. *Colloid Surf. A* **2010**, *360*, 41–46. [[CrossRef](#)]
28. Xue, C.; Guo, X.; Ma, J.; Jia, S. Fabrication of robust and antifouling superhydrophobic surfaces via surface-initiated atom transfer radical polymerization. *ACS. Appl. Mater. Interface* **2015**, *7*, 8251–8259. [[CrossRef](#)] [[PubMed](#)]
29. Block, S.; Hupfield, P.; Itami, Y.; Kitaura, E.; Kleyer, D.; Masutani, T.; Nakai, Y. New Anti-Fingerprint Coatings. *Paint Coat. Industry* **2008**, *24*, 88–92.



© 2018 by the authors. Licensee MDPI, Basel, Switzerland. This article is an open access article distributed under the terms and conditions of the Creative Commons Attribution (CC BY) license (<http://creativecommons.org/licenses/by/4.0/>).